

Membrane Proteomic Responses in Sugar Beet Roots to Salt Stress

Jianing Kang^{1,2,3}, Peng Liao^{1,2}, Bing Yu^{1,2}, Sixue Chen^{1,3}, Haiying Li^{1,2}, Chunquan Ma^{1,2*}

¹Key Laboratory of Molecular Biology of Heilongjiang Province, College of Life Sciences, Heilongjiang University, Harbin 150080, China; ²Engineering Research Center of Agricultural Microbiology Technology, Ministry of Education, Heilongjiang University, Harbin 150080, China; ³Department of Biology, Genetics Institute, Plant Molecular and Cellular Biology Program, University of Florida, Gainesville, FL32610, USA

ABSTRACT

Salt stress as one of the major abiotic stresses limits the world crop production. Sugar beet monosomic addition line M14 is a unique germplasm with salt stress tolerance, and root is directly exposed to salt stress in the soil. Here we report changes in root membrane proteome of the M14 plants in response to 0, 200 mM and 400 mM NaCl treatment using iTRAQ LC-MS/MS quantitative proteomics. A total of 115 differentially expressed membrane proteins (96 increased and 19 decreased) were identified with a significant fold change of >2.0. The proteins were mainly involved in the processes of transport, signaling, stress and defense, energy, protein degradation, and transcription. Transcriptional changes of 10 genes encoding the differential membrane proteins were analyzed using real-time PCR, and seven genes showed a positive correlation between transcriptional and protein levels. These results have revealed interesting mechanisms underlying the M14 root response to the salt stress, which may have potential applications toward improving crop salt tolerance through genetic engineering and molecular breeding.

Keywords: Salt stress; Membrane; Proteomics; LC-MS/MS; Sugar beet M14

INTRODUCTION

Soil salinity has become one of the most serious environmental constraints to crop production [1,2]. Plant response and tolerance to salt stress is a hot topic in current plant biology [3-6]. Salt stress reflects a combination of other stresses, including ionic stress, osmotic stress, and oxidative stress [7-10]. Although different strategies to enhance plant tolerance have been explored, including creating transgenic plants with a limited number of candidate genes, the outcomes have not met expectation and most crops could not grow well on saline soil. Therefore, a comprehensive study of a salt-tolerant crop (e.g., a sugar beet monosomic addition line M14) using omics technologies is important. Proteomics has shown utility in unraveling the molecular mechanisms of plant response to salt stress [11], and the systemic knowledge will greatly facilitate rational engineering and/or breeding for salt tolerance.

The sugar beet line M14 is a unique germline, which was obtained by crossing sugar beet *Beta vulgaris* L. with *B. corolliflora* Zoss. The M14 has the entire 18 chromosomes from *B. vulgaris* L. genome with the addition of chromosome 9 from *B. corolliflora* Z. It exhibits characteristics of apomixes and tolerance to drought, cold and salt stress [12]. Our previous studies have shown that the M14 seedlings can grow under 500 mM NaCl treatment for

7 days without losing viability, making it an interesting material for studying salt stress tolerance [13]. To date, we have made progress in the study of the M14 responses to salt stress at the transcriptomic and proteomic levels [13-16]. Especially, we have studied the changes in leaf membrane proteome of the M14 plants in response to salt stress (0, 200, 400 mM NaCl) and found 40 membrane proteins increased and 10 membrane proteins decreased under salt stress [14]. However, analysis of the leaf membrane proteome of the M14 plants in response to salt stress is inadequate, since we missed the roots, which are the first organ exposed to salt stress [17,18]. Hence, studying root membrane proteome of the M14 plants in response to salt stress is a natural progression toward characterizing root membrane proteins in the M14 tolerance to salt stress.

Plant cell membrane system and many different proteins in or associated with the membranes play important roles in cell functions [19-21]. Especially, the plasma membrane, which separates the environment from the intracellular reactions, is essential for information exchange (signal transduction), material transport, and adaptation to stress conditions [22]. Membrane proteins are certainly important in these processes. Due to the hydrophobicity and low abundance of membrane proteins, it is

Correspondence to: Chunquan Ma, Key Laboratory of Molecular Biology of Heilongjiang Province, College of Life Sciences, Heilongjiang University, Harbin 150080, China, E-mail: chqm@hlju.edu.cn

Received: May 17, 2021, **Accepted:** May 31, 2021, **Published:** June 07, 2021

Citation: Kang J, Liao P, Yu B, Chen S, Li H, Ma C, et al. (2021) Membrane Proteomic Responses in Sugar Beet Roots to Salt Stress. *J Proteomics Bioinform.* 14:541.

Copyright: © 2021 Kang J, et al. This is an open-access article distributed under the terms of the Creative Commons Attribution License, which permits unrestricted use, distribution, and reproduction in any medium, provided the original author and source are credited.

difficult to analyze the membrane proteome using traditional technologies such as 2D gel electrophoresis [23,24]. In this study, we employed a modern iTRAQ LC-MS/MS technology to analyze differentially expressed root membrane proteins of the M14 seedlings in response to salt stress. A total of 115 differentially expressed proteins were identified, with 96 increased and 19 decreased in levels. The proteins were mainly involved in transport, signaling, stress and defense, energy, protein degradation, and transcription. The results have improved understanding of how the M14 plants tolerate salt stress. The resources of the salt stress-related genes and proteins may be applied to improving crop stress tolerance and yield.

MATERIALS AND METHODS

Plant materials and NaCl treatment

Sugar beet monosomic additional line M14 seeds were sown and grown on vermiculite, and then the seedlings were transferred to Hoagland solution. They were grown in a growth chamber under a 14 h/10 h light/dark photoperiod ($450 \mu\text{mol m}^{-2}\text{s}^{-1}$ PAR) at 25°C/20°C (day/night) and 65% relative humidity. Five-week-old plants were divided into three groups, i.e., control group (without NaCl), 200 mM NaCl treatment group, and 400 mM NaCl treatment group. The plants were treated for 7 days. The NaCl concentrations were chosen according to our previous report showing that the M14 plants can tolerate up to 500 mM NaCl [13]. Plant materials were harvested directly into liquid nitrogen and stored in -80°C freezer. Three biological replicates were collected for each sample [25-33].

Physiological and biochemical analyses of control and salt-stressed roots

Root relative water content (RWC). After different concentrations of salt treatment, fresh weight was measured immediately after roots were harvested, and dry weight was obtained after the samples were dried at 75°C for 48 h. Turgor weight was determined by subjecting leaves to rehydration for 2 h after their dry weight was measured. The RWC was determined according to a previous method: $\text{RWC (\%)} = (\text{fresh weight} - \text{dry weight}) / (\text{turgor weight} - \text{dry weight}) \times 100$.

Membrane permeability: Membrane permeability was assessed by electrolyte leakage (EL). Root samples from different treatments (0, 200 mM, 400 mM NaCl) were rinsed three times with deionized water and placed in a tube containing 10 mL of deionized water. The tubes were placed in a vacuum chamber until the roots became wilted. The initial electrical conductivity of the solution (EC1) was determined. After autoclaving the tubes at 120°C for 30 min, the final electrical conductivity (EC2) was obtained. EL was calculated as a percentage of EC1/EC2.

SOD activity: One-gram root material was ground in 2 mL 50 mM phosphate buffer (pH 7.8) with 1 × protease inhibitor cocktail. After centrifugation at 4°C 12000 rpm for 10 min, the supernatant was used for SOD activity assay. Three biological replicates were prepared for each sample. The SOD activity was

assayed by measuring the inhibition of photochemical reduction of nitro blue tetrazolium (NBT) using a spectrophotometer at 560 nm as previously described. The 3 mL reaction mixture contained 50 mM phosphate buffer (pH 7.8), 13 μM methionine, 63 μM NBT, 1.3 μM riboflavin and 100 μL enzyme extract. One unit of SOD activity was defined as the amount of enzyme required to cause 50% inhibition of NBT reduction.

Microsomal membrane protein extraction

A total of 50 g fresh roots were harvested from control, 200 mM and 400 mM NaCl treated samples. Each sample was ground into a fine powder in liquid nitrogen, followed by suspension and grinding in 15 ml of homogenization buffer (10 mM Tris-HCl pH7.4, 10 mM KCl, 1.5 mM MgCl₂, 10 mM DTT, 0.5 M Sucrose, and 1 mM PMSF). The resulting slurry was filtered through four layers of cheesecloth, and the filtered homogenate was centrifuged at 4°C, 800 g for 10 min to remove debris. The supernatant was transferred to an ultracentrifuge tube and centrifuged at 4°C, 100,000 g for 1.5 h. The microsomal pellet was washed with cold 100 mM Na₂CO₃ and homogenized with a Dounce homogenizer. The homogenate was centrifuged again at 4°C, 100,000 g for 1.5 h. The microsomal pellet was collected with 500 μL resuspension buffer (100 mM HEPES pH7.0, 0.05% Triton X-100 and 0.5 M Sucrose) and centrifuged at 4°C, 800g for 10 min. The supernatant microsome was carefully transferred to a new eppendorf tube and kept at -80°C. The protein concentration was estimated using a Bradford Protein Assay Kit according to the manufacturer's instructions (Sigma, USA).

SDS-PAGE and western blot analysis

Protein samples of 15 μg microsomal protein each were loaded onto SDS polyacrylamide gels. The gel was blotted to PVDF membrane (146 mA, 2.5 h) and probed with primary antibodies against aquaporin (1:1000 dilution) and actin (1:5000 dilution) (Agrisera Inc., Sweden) for 2 h at room temperature. The blot was washed four times with a TBST solution (200 mM Tris-HCl pH 7.6, 137 mM NaCl and 0.05% Tween 20, v/v), and then incubated with a secondary antibody (goat-anti-rabbit IgG horse radish peroxidase conjugated, at 1:5000 dilutions, Zhong Shan Jin Qiao Inc., China) for 1 h at room temperature. The blot was finally washed with the TBST and a TBS solution (200 mM Tris-HCl pH 7.6 and 137 mM NaCl), and then developed using a DAB Kit (Zhong Shan Jin Qiao Inc., China). A replicate protein gel was stained with Coomassie Brilliant Blue R-250 for equal loading control.

iTRAQ labeling and LC-MS/MS identification

The acetone pellets of the microsome preparations from control, 200 mM NaCl treated and 400 mM NaCl treated samples (each of 100 μg protein) were collected by centrifugation at 20,000g, 4°C and dissolved in 1% SDS, 100 mM triethylammonium bicarbonate, pH 8.5. Reduction, alkylation, trypsin digestion and peptide labeling were conducted using the iTRAQ 8-plex reagent kit following the manufacturer's instructions (AB Sciex Inc.,

Framingham, MA, USA). The control replicates were labeled with iTRAQ tags 113, 114 and 115; the 200 mM NaCl replicates with tags 116 and 117; and the 400 mM NaCl replicates with tags 118, 119, and 121. The labeled microsomal peptides were desalted by C18-solid phase extraction and dissolved in strong cation exchange (SCX) solvent A (25% (v/v) acetonitrile, 10 mM ammonium formate, and 0.1% (v/v) formic acid, pH 2.8). The peptides were fractionated using an Agilent high-performance liquid chromatographer (HPLC) 1260 with a polysulfethyl A column (2.1 × 100 mm², 5 μm, 300 Å; PolyLC, Columbia, MD, USA). Peptides were eluted with a linear gradient of 0–20% solvent B (25% (v/v) acetonitrile and 500 mM ammonium formate, pH 6.8) over 60 min followed by ramping up to 100% solvent B in 5 min. The absorbance at 280 nm was monitored, and a total of 16 fractions were collected. The fractions were lyophilized and resuspended in LC solvent A (0.1% formic acid in 97% water (v/v), 3% acetonitrile (v/v)). A quadrupole Orbitrap (Q Exactive) mass spectrometry (MS) system (Thermo Fisher Scientific, Bremen, Germany) is used to identify the labeled peptides. The instrument was run in a data-dependent mode with a full MS (400–2000 m/z) resolution of 70 000 and five MS/MS experiments using high energy collision dissociation at a normalized collision energy of 28%. The isolation width was 3 Th, and the AGC target was 1e6. Each sample fraction was loaded onto an Easy-nLC 1000 system (Thermo Fisher Scientific, Bremen, Germany), which flows at 300 nL/min during a linear gradient from solvent A (0.1% formic acid (v/v)) to 30% solvent B (0.1% formic acid (v/v)) for 80 min and to 99.9% acetonitrile (v/v) for an additional 10 min.

Analysis of differentially expressed proteins

The iTRAQ MS/MS data were processed by a thorough database searching considering biological modification and amino acid substitution against a non-redundant *B. vulgaris* database (53,260 entries) with Proteome Discoverer v1.4 (Thermo Fisher Scientific, Bremen, Germany). A differentially expressed protein must have at least three confident MS/MS spectra (1% FDR) and a p-value < 0.05 with fold change thresholds (< 0.5 or > 2.0). Functions and known subcellular localizations of the identified proteins were inferred from the UniProt (<http://www.ebi.uniprot.org/index>) and literature.

Unknown subcellular localization was predicted using Plant-mPLoc (<http://www.csbio.sjtu.edu.cn/bioinf/plant-multi/>) and TargetP 1.1 (<http://www.cbs.dtu.dk/services/TargetP/>). Prediction of protein transmembrane helices was conducted using the TMHMM Server v. 2.0 (<http://genome.cbs.dtu.dk/services/TMHMM-2.0/>). Pathways related to the differentially expressed proteins were obtained from KEGG pathway database (<http://www.kegg.jp/>).

Quantitative real-time PCR (qRT-PCR) analysis

Total RNA was isolated from the frozen samples using a TRIZOL reagent (Invitrogen Inc., USA). After removing genomic DNA

using DNase I, cDNA was synthesized using a PrimeScript RT Reagent Kit (TaKaRa, Shiga, Japan). Gene specific primers of selected proteins were designed using online Primer3 Plus. Quantitative RT-PCR was performed in a 20 μL mixture containing 10 μL 2 × SYBR[®] Premix Ex Taq[™] (TaKaRa, Shiga, Japan), 2 μL cDNA, 0.3 μL gene-specific primers, and 7.7 μL double distilled H₂O. The PCR conditions were: 95°C for 3 min; 95°C for 15 s, 61°C for 30 s, 40 cycles, on a CFX96 Real-Time PCR Detection System (Bio-Rad Inc., USA). Three biological replicates were used for each sample. All the data were analyzed using CFX Manager software (Bio-Rad Inc.) and the delta CT method was used for quantification.

Metabolite measurement

Cellular glucose was assayed using a Glucose (GO) Assay Kit following the manufacturer's instructions (Sigma-aldrich, USA). Briefly, glucose is oxidized to gluconic acid and hydrogen peroxide by glucose oxidase. Hydrogen peroxide reacts with o-dianisidine in the presence of peroxidase to form a colored product, which reacts with sulfuric acid to form a more stable colored product. The intensity of the pink color was measured at 540 nm, which is proportional to the original glucose concentration. The content of reduced glutathione (GSH) was measured based on the increase of absorbance at 412 nm when 5,5'-dithiobis-(2-nitrobenzoic acid) was reduced by GSH using the published methods.

RESULTS AND DISCUSSION

Morphological, physiological, and biochemical responses to salt stress

To determine how salt stress affects the M14 seedlings, we inspected their morphological responses to different NaCl concentrations (0, 200 mM and 400 mM NaCl). As shown in Figure 1A, the M14 seedlings under 200 mM and 400 mM NaCl treatment grew slowly, and the fully expanded leaves appeared slightly chlorotic as compared with the control plants. The growth inhibition under the 400 mM NaCl treatment was marked, but the seedlings could survive the 400 mM NaCl treatment for seven days. The root length was also decreased with the increasing salt concentrations (Figure 1B). These results are consistent with our previous observation [15].

In addition to morphological changes, relative water content (RWC) and membrane permeability of the M14 roots were affected by the salt stress. Compared with the control, RWC of the M14 roots under 200 mM and 400 mM NaCl treatment decreased by 12.37% and 28.46%, respectively (Figure 2A). Salt stress caused membrane permeability to increase and then intracellular electrolyte to leak. As shown in Figure 2B, electrolyte leakage (EL) under 200 mM and 400 mM NaCl treatments increased by 8.86% and 20.88%, respectively, compared with the control. As part of the salt stress response, SOD activity increased after the salt treatments (Figure 2C).



Figure 1: Morphological changes of sugar beet M14 seedlings under 0, 200 mM, 400 mM NaCl treatments A. Phenotype of sugar beet M14 seedlings. B. Root length of sugar beet M14 seedlings.

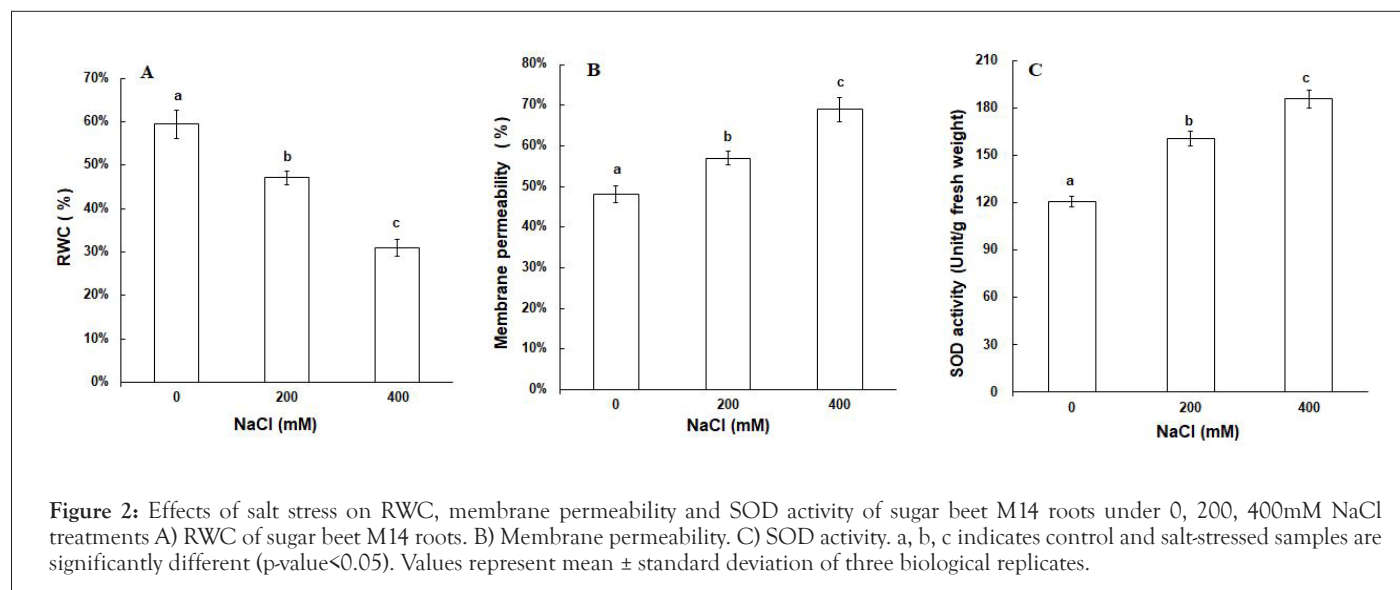


Figure 2: Effects of salt stress on RWC, membrane permeability and SOD activity of sugar beet M14 roots under 0, 200, 400mM NaCl treatments A) RWC of sugar beet M14 roots. B) Membrane permeability. C) SOD activity. a, b, c indicates control and salt-stressed samples are significantly different (p-value<0.05). Values represent mean ± standard deviation of three biological replicates.

Evaluation of microsomal membrane purity

Western blotting was used to evaluate the purity of the microsomal membrane preparations. PIP proteins are aquaporins that regulate the transport of water and small neutral molecules across cell membrane [33]. Actin is a family of globular proteins that form microfilaments in the cytoplasm [34]. The antibodies against PIP1 and actin were used to evaluate the relative purity of the microsomal membrane preparations and soluble protein extracts. As shown in Figure 3A, there was an obvious band of PIP1 (~ 28 kDa) in the different membrane preparations, but not detectable in the soluble protein extracts. As to actin, we detected the signal in the microsomal membrane preparations, but the level is significantly lower than in the soluble protein extract (Figure 3B). Although the microsomes were prepared using ultra-high-speed centrifugation and washed repeatedly with Na_2CO_3 , it is possible that small number of soluble proteins was trapped in the vesicles. Based on these results, the microsomal membrane preparations were highly enriched for the membrane proteomics experiments.

Differentially expressed membrane proteins of M14 roots in response to salt stress

Using the iTRAQ labeling and two-dimensional LC-MS/MS approach, a total of 343 differentially expressed proteins were identified at a 99% confidence level. These proteins were significantly increased or decreased (a fold change >2.0 or <0.5 , $p < 0.05$) in response to the NaCl treatments. Prediction of transmembrane helices in the identified proteins showed that 115 of the 343 proteins had one or more transmembrane domains

(TMDs) (Table 1, Supplemental Table 1). This result suggests that many proteins in our membrane preparations may be peripheral membrane proteins or membrane associated proteins in spite of extensive washing steps with sodium bicarbonate.

We predicted the subcellular location of the 115 differentially expressed membrane proteins. These proteins are mainly located in nucleus, vacuole and plasma membrane (Figure 4A). Based on their function categories in Uniprot and literature (Figure 4B), these proteins fell into nine groups, including metabolism, transport, cellular structure, degradation, energy, signaling, stress and defense, transcription related and unknown. The majority of the proteins (32%) were transport-related. The other differentially expressed membrane proteins were classified into metabolism (28%), cellular structure (8%), signaling (7%), stress and defense (6%), energy (4%), degradation (4%), transcription related (4%) and unknown (7%).

Comparison of the proteome data with transcriptome and metabolite data

To determine whether gene transcription level changes correlated with the protein level changes, we selected 10 genes encoding the M14 differentially expressed membrane proteins and analyzed their transcriptional changes using real-time PCR (Figure 5). Overall, seven genes showed a positive correlation between transcriptional and protein levels. Three genes showed different patterns between transcriptional and protein levels, i.e., glutamate receptor protein, glucose-6-phosphate translocator and sucrose transporter 4 showed opposite trends in transcript and protein levels (Table 2).

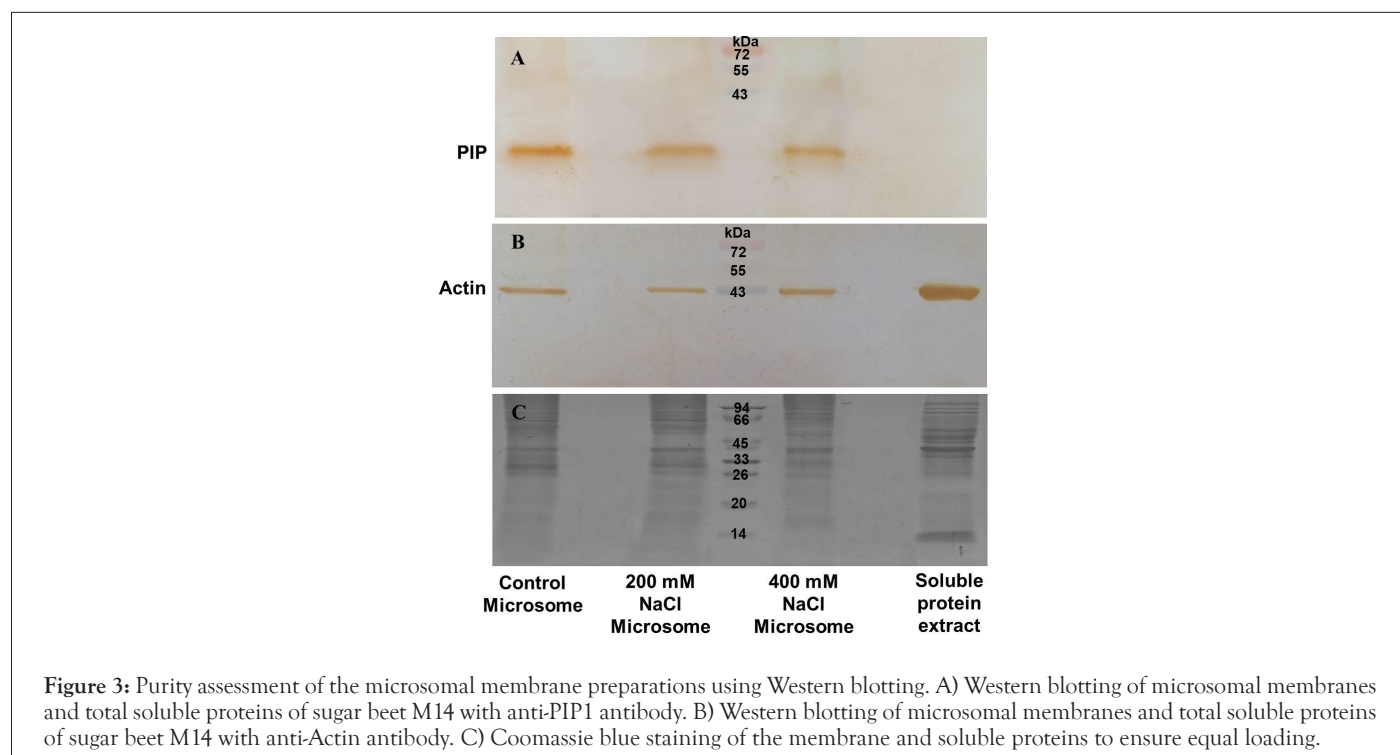


Figure 3: Purity assessment of the microsomal membrane preparations using Western blotting. A) Western blotting of microsomal membranes and total soluble proteins of sugar beet M14 with anti-PIP1 antibody. B) Western blotting of microsomal membranes and total soluble proteins of sugar beet M14 with anti-Actin antibody. C) Coomassie blue staining of the membrane and soluble proteins to ensure equal loading.

Table 1: Proteins identified and quantified in the microsomal membrane preparations from the control and NaCl treated sugar beet M14 using iTRAQ LC-MS/MS.

Accessiona	Protein nameb	Scorec	Unique Peptidesd	PSMe	200 mM/ control p_valuefg	400 mM/ control p_valuef	Protein locationg	TMDh
Transport								
gi 1402833	Plasma membrane major intrinsic protein	105.46	7	32	0.38/0.00	0.46/0.00	Cell membrane	6
gi 4884866	Water channel protein MipI	21.16	2	4	0.33/0.00	0.35/0.00	Vacuole	6
gi 5911732	Delta tonoplast intrinsic protein	5.54	2	4	0.28/0.00	0.4/0.00	Vacuole	6
gi 224142179	Sugar carrier family protein	2.88	2	2	0.3/0.01	0.32/0.00	Cell membrane	11
gi 357448857	Transmembrane protein, putative	3.57	2	2	2.74/0.05	2.82/0.04	Nucleus	1
gi 375273925	ABCG/PDR subfamily ABC protein	25.59	5	10	–	3.19/0.02	Cell membrane	13
gi 566191430	Organic cation transporter-related protein	18.59	3	5	0.44/0.00	0.5/0.01	Cell membrane	4
gi 590563830	Tonoplast intrinsic protein 1,3	89.3	3	24	0.2/0.00	0.48/0.00	Vacuole	6
gi 590571602	Glutamate receptor	52.78	2	13	2.07/0.00	1.97/0.00	Cell membrane	3
gi 590596544	Sucrose proton symporter 4	3.98	2	4	0.18/0.02	0.22/0.03	Cell membrane	5
gi 590605090	Got1/Sft2-like vesicle transport protein	3.85	2	5	2.19/0.00	–	Cell membrane	4
gi 731366334	Choline transporter-like protein 2	3.25	2	2	0.48/0.00	0.46/0.00	Cell membrane	10
gi 590657813	Adenine nucleotide carrier 1 isoform 2	9.31	5	23	1.47/0.05	2.44/0.01	Mitochondrion	p
gi 590686906	Na ⁺ /H ⁺ antiporter 1 isoform 1	2.56	2	2	–	2.01/0.00	Plastid/Chloroplast	9
gi 104891884	Transmembrane emp24 domain-containing	4.77	2	4	1.87/0.04	2.04/0.00	Nucleus	1
gi 757114677	Potassium transporter	44.89	7	18	0.31/0.00	0.32/0.00	Miscellaneous	11
gi 117622284	Apyrase-like protein	4.42	2	2	2.29/0.00	–	Others	1
gi 4322319	Ammonium transporter	28.25	2	5	4.021/0.03	7.269/0.00	Miscellaneous	6
gi 728845684	Acyl-CoA-binding domain-containing 5-like	3.29	2	3	0.4/0.00	0.49/0.00	Nucleus	1
gi 590657945	Sugar transport protein 13	25.5	2	4	3.131/0.00	3.546/0.00	Cell membrane	12
gi 9295277	Glucose-6P/phosphate translocator precursor	9.05	2	3	0.39/0.01	0.47/0.00	Others	7
gi 566162088	Nitrate transporter family protein	2.27	2	3	0.31/0.00	0.21/0.00	Vacuole	8
gi 9295275	Phosphoenolpyruvate/phosphate translocator	20.44	2	5	0.39/0.00	0.39/0.00	Plastid/Chloroplast	7
gi 731376782	Mechanosensitive ion channel protein 6-like	8.26	2	3	1.12/0.03	2.36/0.00	Nucleus	6
gi 1050565596	25.3 kDa vesicle transport protein	22.83	2	5	4.344/0.00	3.62/0.00	Endoplasmic reticulum	1
gi 508728355	Sec23/Sec24 protein transport isoform 1	23.49	2	6	4.138/0.00	4.108/0.00	Golgi apparatus	1
gi 87248025	Cytochrome oxidase subunit 2	16.47	3	7	3.582/0.00	5.056/0.00	Mitochondrion	2

gi 1063015814	Translocation protein sec62	11.42	3	5	2.506/0.01	2.055/0.01	Nucleus	3
gi 5881115	Glucose transporter	33.55	2	7	4.977/0.00	4.513/0.00	Cell membrane	5
gi 162681975	Phospholipid-transporting ATPase	19.56	2	4	3.249/0.00	4.238/0.00	Cell membrane	8
gi 15234277	Cation transporter/ E1-E2 ATPase	23.64	3	14	2.546/0.00	2.15/0.00	Cell membrane	9
gi 15225747	H ⁺ -ATPase 6	139.37	6	48	2.039/0.00	2.458/0.00	Cell membrane	9
gi 1063018254	ABC transporter A family member 7	22.48	4	7	2.138/0.01	4.296/0.00	Cell membrane	7
gi 1050580066	ABC transporter B family member 19	10.95	2	5	3.021/0.01	2.152/0.03	Cell membrane	10
gi 1063510884	ABC transporter G family member 35	19.93	3	8	1.79/0.03	2.365/0.00	Cell membrane	13
gi 672190336	ABC transporter C family member 2	63.89	2	13	4.588/0.01	3.703/0.01	Vacuole	14
gi 1052190224	ABC transporter C family member 14	14.37	2	7	3.548/0.01	3.945/0.00	Cell membrane	15
Metabolism								
gi 350534796	Beta-glucosidase 08	2.14	2	5	2.14/0.05	1.7/0.00	Cell membrane	1
gi 566161131	Lecithin:cholesterol acyltransferase	4.49	2	2	1.82/0.04	2.88/0.01	Mitochondrion	1
gi 566232333	Beta-D-glucan exohydrolase family protein	20.69	2	6	2.47/0.00	–	Miscellaneous	1
gi 672117420	NADPH-cytochrome P450 reductase	7.52	2	2	7.639/0.00	5.42/0.00	Endoplasmic reticulum	1
gi 11386885	Hexokinase-1 (EC 2.7.1.1) (NtHxK1)	19.71	3	4	2.48/0.00	1.87/0.00	Mitochondrion	1
gi 590703969	Dolichyl-diphosphooligosaccharide glycosyltransferase	25.82	3	7	2.09/0.00	1.53/0.03	Cell membrane	2
gi 745790929	Cytochrome P450 CYP73A120	148.31	2	39	1.73/0.00	2.34/0.00	Endoplasmic reticulum	p
gi 5381253	Peroxidase	68.97	10	23	1.5/0.00	2.21/0.00	Cytoplasm	1
gi 1050648053	Peroxidase 12	19.38	2	3	7.541/0.00	4.747/0.01	Vacuole	1
gi 922392058	Cytochrome P450 family 72 protein	5.65	2	2	0.47/0.01	0.33/0.00	Endoplasmic reticulum	1
gi 590628218	Electron transport SCO1/SenC family protein	8.49	2	2	0.44/0.00	0.36/0.00	Nucleus	1
gi 590634954	Calcium-dependent phosphotriesterase	4.26	2	2	2.16/0.00	2.35/0.00	Vacuole	1
gi 731358483	Squalene synthase-like	12.01	2	2	2.16/0.00	2.91/0.00	Endoplasmic reticulum	1
gi 1063526228	Serine carboxypeptidase-like	11	3	6	6.608/0.00	4.19/0.00	Miscellaneous	1
gi 672134872	Dihydrolipoyllysine-residue succinyltransferase	6.51	3	3	6.282/0.00	4.226/0.00	Mitochondrion	1
gi 672147003	Calnexin	23.62	3	6	5.054/0.02	2.453/0.02	Endoplasmic reticulum	1
gi 1063488914	3-ketoacyl-CoA thiolase 2	51.62	4	17	4.93/0.00	4.112/0.00	Peroxisome	1
gi 1063682700	Aspartic proteinase A1	10.47	2	2	4.033/0.02	6.647/0.00	Vacuole	1
gi 15227109	UDP-xylose synthase 4	21.1	3	9	3.498/0.01	2.828/0.01	Golgi apparatus	1

gi 1063472093	Leucine-rich repeat protein kinase TMK3	7.15	2	4	3.466/0.00	3.257/0.00	Cell membrane	1
gi 15224857	Hexokinase 2	41.29	4	17	3.455/0.00	3.52/0.00	Mitochondrion	1
gi 1050616617	NADH-cytochrome b5 reductase 1	47.07	2	13	2.81/0.01	3.27/0.00	Mitochondrion	1
gi 672181971	Somatic embryogenesis receptor kinase 2	27.53	2	9	2.597/0.00	2.537/0.00	Cell membrane	1
gi 672183947	UDP-glucuronic acid decarboxylase 2	18.55	3	6	2.513/0.01	3.368/0.00	Golgi apparatus	1
gi 15222955	Sterol methyltransferase 3	20.51	2	6	2.436/0.04	2.245/0.04	Cytoplasm	1
gi 1050571659	Calcium ion-binding protein	3.65	2	2	2.303/0.02	3.079/0.00	Nucleus	1
gi 79324537	Leucine-rich repeat protein kinase family	6.44	2	2	2.078/0.01	2.009/0.00	Cell membrane	1
gi 590714186	Putative kinase-like protein TMKL1	11.92	2	3	3.858/0.00	3.773/0.00	Cell membrane	2
gi 124360660	C2 calcium/lipid-binding and GRAM domain	12.21	2	4	2.816/0.01	3.631/0.00	Cytoplasm	2
gi 508714531	Chromatin-remodeling protein 11 isoform 2,	8.47	3	4	1.694/0.03	2.917/0.00	Nucleus	2
gi 508774440	H ⁺ -transporting ATPase	110.12	2	33	2.866/0.00	4.381/0.00	Cell membrane	9
gi 30693010	Dolichyl-diphosphooligosaccharide-protein glycosyltransferase	5.11	3	11	3.945/0.01	5.561/0.00	Cell membrane	11
Cellular structure								
gi 960513859	Disulfide-isomerase like 2-1 precursor	85	9	23	–	2.04/0.04	Endoplasmic reticulum	1
gi 312837047	Fasciclin-like arabinogalactan protein	49.57	5	13	1.13/0.04	2/0.03	Cell membrane	P
gi 15230120	Leucine-rich repeat extensin-like protein 4	10.36	3	3	2.23/0.02	2.34/0.00	Cell wall	1
gi 1063686221	Microtubule-associated proteins 70-2	18.58	3	4	4.111/0.00	3.537/0.00	Nucleus	1
gi 1063051750	Cytochrome b5	15.96	3	3	3.144/0.00	3.158/0.00	Endoplasmic reticulum	1
gi 508715008	Plant snare 13 isoform 1	20	3	7	2.636/0.00	3.663/0.00	Miscellaneous	1
gi 590657272	NADH dehydrogenase subunit 13-A	11.56	3	5	2.482/0.04	2.272/0.04	Nucleus	1
gi 15237846	GPI-anchored adhesin-like protein	3.36	2	2	2.304/0.03	2.65/0.01	Nucleus	1
gi 1063515388	Callose synthase 8 isoform X1	7.19	2	2	2.581/0.03	3.75/0.00	Cell wall	15
Degradation								
gi 731355241	Transmembrane E3 ubiquitin-protein ligase 1	0	2	2	2.2/0.00	2.63/0.00	Miscellaneous	7
gi 731344029	Miraculin-like protein	3.38	2	2	–	6.92/0.00	Vacuole	1
gi 590638321	Kunitz family trypsin and protease inhibitor	20.01	4	5	1.45/0.02	2.74/0.00	Vacuole	1
gi 731364471	Trypsin inhibitor BvTI-like	13.67	3	5	0.73/0.03	2.03/0.04	Vacuole	1
gi 731344067	Trypsin inhibitor-like	66.54	2	19	3.64/0.00	3.6/0.00	Vacuole	P
Energy								

gi 162279934	ATPase subunit 8	19.74	3	6	0.34/0.00	0.4/0.00	Mitochondrion	P
gi 590628122	Thiamine pyrophosphate pyruvate decarboxylase	88.18	2	24	1.87/0.00	2.72/0.00	Others	P
gi 566206055	AAA-type ATPase family protein	136.94	12	36	2.05/0.00	1.53/0.01	Nucleus	1
gi 733214298	V-type proton ATPase	33.56	2	9	1.59/0.00	2.71/0.01	Vacuole	4
gi 1063021722	Luminal-binding protein 5	200.99	3	65	7.171/0.01	4.723/0.00	Miscellaneous	1
Signaling								
gi 566182885	Calcium-binding EF hand family protein	30.57	5	7	2.5/0.00	1.36/0.04	Nucleus	1
gi 357453013	Gland-specific fatty acyl-CoA reductase	8.49	4	6	2.25/0.00	3.28/0.00	Golgi apparatus	1
gi 590704059	Ppeptidoglycan-binding LysM domain-protein	4.26	2	2	—	2.66/0.00	Miscellaneous	2
gi 1052180221	Calcium-transporting ATPase	8.74	2	4	2.603/0.05	3.182/0.02	Endoplasmic reticulum	8
gi 914726339	Lectin receptor kinase	2.39	2	2	1.83/0.00	2.6/0.00	Miscellaneous	2
gi 590673018	Calcium-dependent lipid-binding family protein	32.42	2	8	1.21/0.03	2.3/0.01	Cytoplasm	1
gi 870858158	Hypothetical protein BVRB_6g131340	21.42	3	6	—	2.02/0.00	Nucleus	2
gi 1063731028	Leucine-rich repeat transmembrane kinase	25.81	3	5	3.95/0.00	4.142/0.00	Cell membrane	1
Stress and defense								
gi 590576462	Gamma-glutamyl transpeptidase 4	0	2	5	2.54/0.00	—	Cytoplasm	2
gi 590632582	Short chain alcohol dehydrogenase	5.16	2	2	0.43/0.00	0.32/0.00	Others	1
gi 731312085	Putative germin-like protein 2-1	16.26	2	5	2.33/0.02	1.53/0.03	Cell wall	1
gi 731355175	Cytochrome b561 and DOMON domain protein	5.1	2	2	7.57/0.01	9.5/0.00	Cell membrane	6
gi 731363857	Uncharacterized protein LOC104906584	10.43	3	3	2.18/0.01	1.82/0.01	Nucleus	1
gi 590691184	Prohibitin-1	22.48	2	7	3.415/0.00	2.977/0.00	Mitochondrion	1
gi 508775253	Gamma carbonic anhydrase	10.02	2	5	3.108/0.05	3.205/0.02	Mitochondrion	1
Transcription-related								
gi 590682236	ATP-dependent RNA helicase, isoform 1	8.32	3	9	2.09/0.00	1.6/0.00	Nucleus	P
gi 590722100	Mediator of RNA polymerase II subunit 12	0	5	8	2.1/0.02	—	Others	P
gi 922333194	ORMDL family protein	1.78	2	4	0.36/0.00	0.43/0.00	Miscellaneous	3
gi 922355988	RING-H2 zinc finger protein	0	8	12	2.56/0.00	—	Nucleus	1
Unknown								
gi 870843088	Hypothetical protein BVRB_9g225960	3.16	2	2	0.37/0.00	0.48/0.01	Secretory pathway	1

gi 731354114	Uncharacterized protein LOC104902356	7.16	2	4	—	3.16/0.00	Nucleus	2
gi 590699330	Quasimodo2 like 2 isoform 2	0	2	2	—	2.27/0.00	Cytoplasm	1
gi 628819133	Unknown	27.88	5	6	2.32/0.00	1.84/0.00	Mitochondrion	5
gi 827346383	Unknown	15.72	2	3	2.25/0.00	—	Plastid/Chloroplast	1
gi 870863566	Hypothetical protein BVRB_4g074950	27.13	3	8	2.35/0.00	—	Cell membrane	1
gi 731370131	PREDICTED: SEC12-like protein 1	13.16	2	4	2/0.00	1.47/0.02	Nucleus	1
gi 307543176	Unknown	151.39	3	39	2.21/0.00	1.3/0.05	Secretory pathway	2

a: Protein gi number from NCBI; b: Name of the protein identified by MS/MS; c: Peptide match score summation; d: The number of specific peptides in the protein group; e: The peptide-spectrum matches; f: Average ratio from confident changes in different replicates; g: Predicting subcellular localization of plant proteins; h: Predicted number of TMD (transmembrane domain) (P, probable).

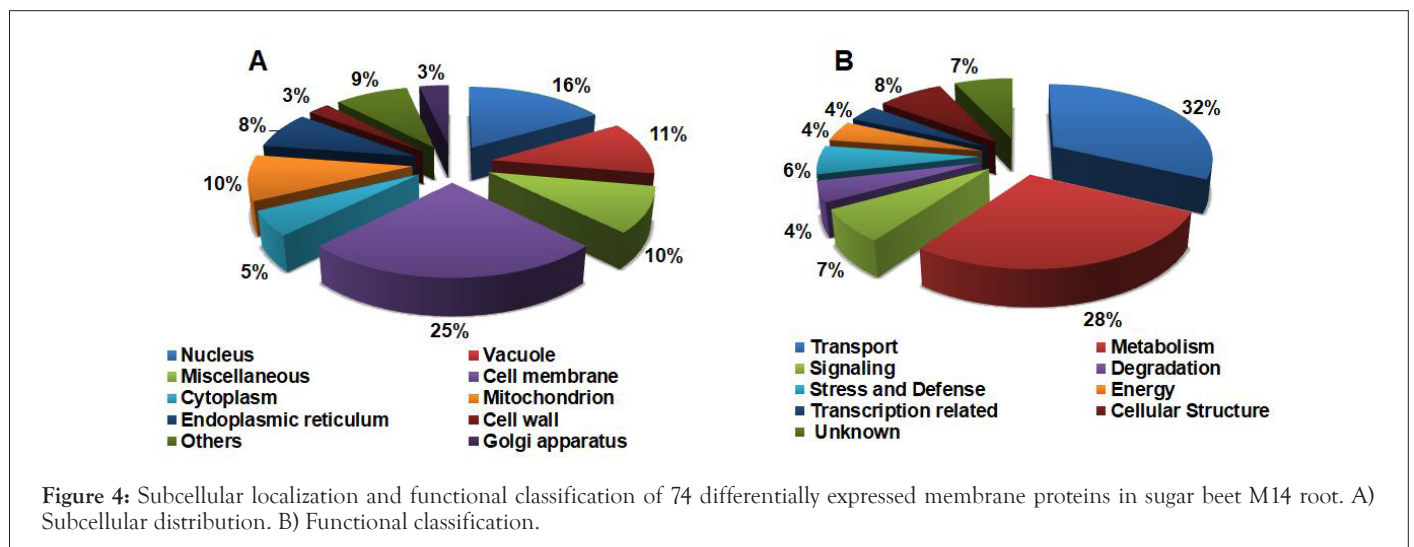


Figure 4: Subcellular localization and functional classification of 74 differentially expressed membrane proteins in sugar beet M14 root. A) Subcellular distribution. B) Functional classification.

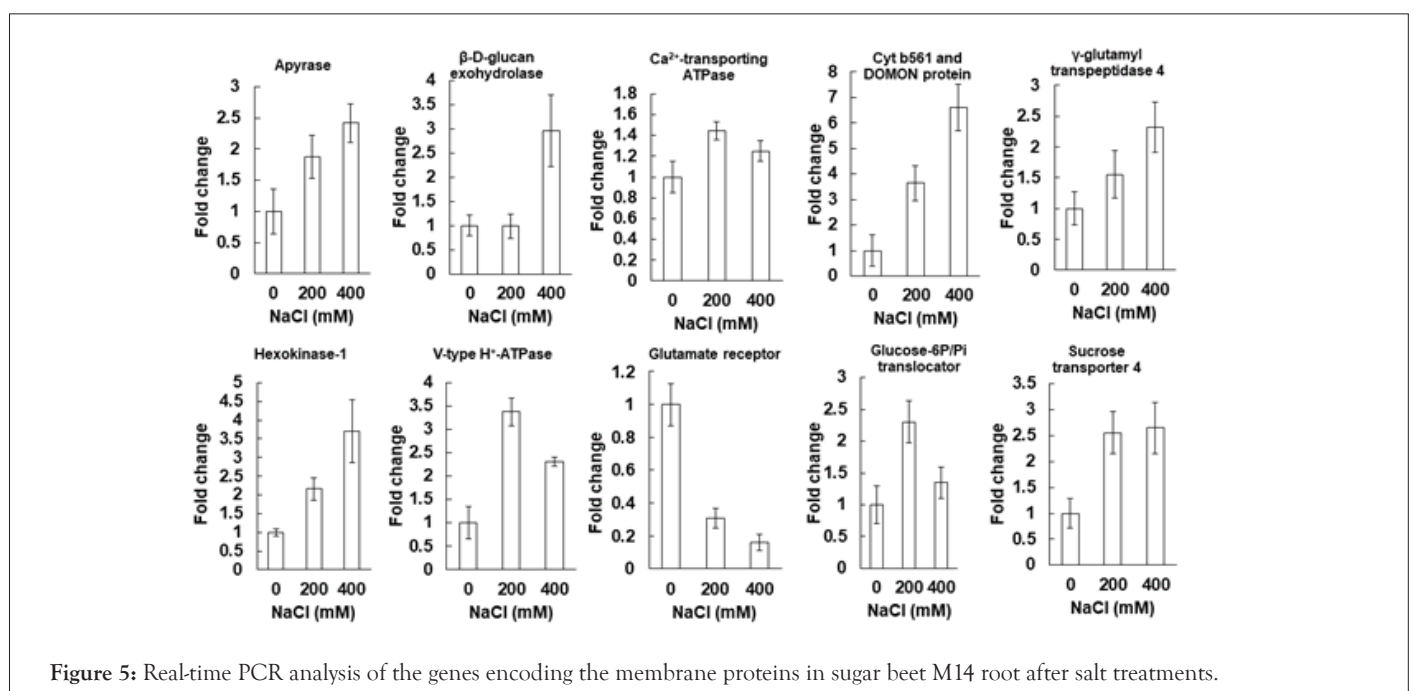


Figure 5: Real-time PCR analysis of the genes encoding the membrane proteins in sugar beet M14 root after salt treatments.

Table 2: Comparison of the transcriptional level and protein level of the differentially expressed root membrane proteins.

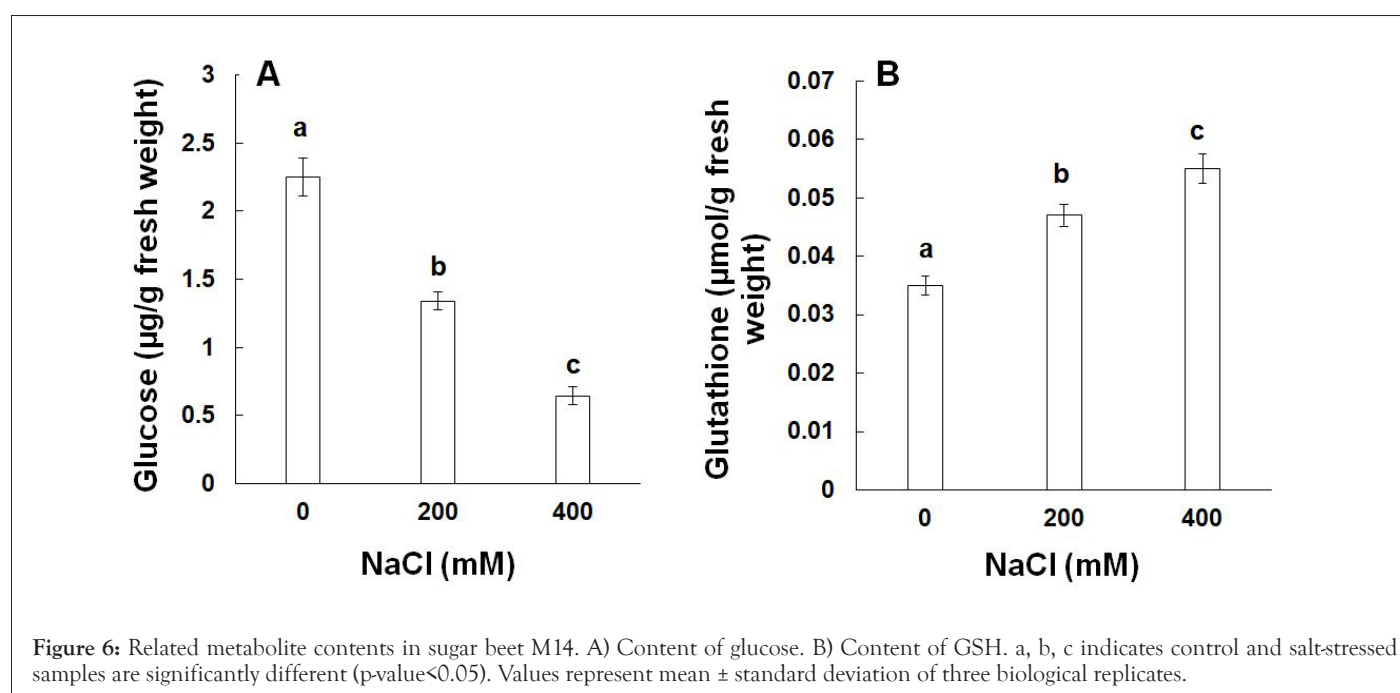
No.	Protein ID ^a	Protein name	RT-PCR ^b (200 mM/control) (400 mM/control)		Protein abundance ^c (200 mM/control) (400 mM/control)	
1	gi 566232333	Beta-D-glucan exohydrolase	↑1.3	↑3.0	↑2.5	—
2	gi 590571602	Glutamate receptor	↓0.3	↓0.2	↑2.0	↑2.0
3	gi 9295277	Glucose-6P/phosphate translocator	↑2.3	↑1.4	↓0.4	↓0.5
4	gi 11386885	Hexokinase-1	↑2.2	↑3.7	↑2.5	↑1.9
5	gi 117622284	Apyrase	↑1.9	↑2.4	↑2.3	↑1.0
6	gi 590576462	Gamma-glutamyl transpeptidase 4	↑1.6	↑2.3	↑2.5	↑1.1
7	gi 731355175	Cytochrome b561 and DOMON domain-containing protein	↑3.6	↑6.6	↑7.6	↑9.5
8	gi 590596544	Sucrose proton symporter	↑2.6	↑2.7	↓0.2	↓0.2
9	gi 733214298	V-type proton ATPase	↑3.4	↑2.3	↑1.6	↑2.7
10	gi 674961184	Calcium-transporting ATPase	↑1.4	↑1.3	↑2.8	↑1.2

A: gi number of NCBI; b: transcript level (NaCl treatment/control); c: protein level (NaCl treatment/control).

— no change; ↓ decreased; ↑ increased.

We measured the contents of glucose and glutathione (GSH) in the samples. With the increase of salt concentration, glucose content in the M14 roots gradually decreased. Strikingly, glucose content dropped more than 70% under 400 mM salt treatment compared with control (Figure 6). In the metabolic pathway (Figure 7), beta-D-glucan exohydrolase (gi|566232333) increased under 200 mM salt treatment. However, there is no direct correlation between this enzyme and glucose content, indicating other pathways may affect the glucose content. GSH is an important antioxidant in plant cells, preventing damage to important cellular components caused by excessive production of reactive oxygen species [35].

With the increased of salt concentration, GSH concentration increased, e.g., by 25% in the 400mM salt treatment (Figure 6). Glutamate receptor protein (gi|590571602) also increased in the 200 mM and 400 mM NaCl treatments with similar trend, indicating that the glutamate receptor protein might contribute to the increase of GSH under the salt treatments (Figure 7). Interestingly, in *Arabidopsis* innate immunity response, a glutamate receptor was found to mediate GSH trigger calcium transients and transcriptional changes [36]. The functions of the M14 glutamate receptor and GSH in salt stress response are to be investigated in future studies.



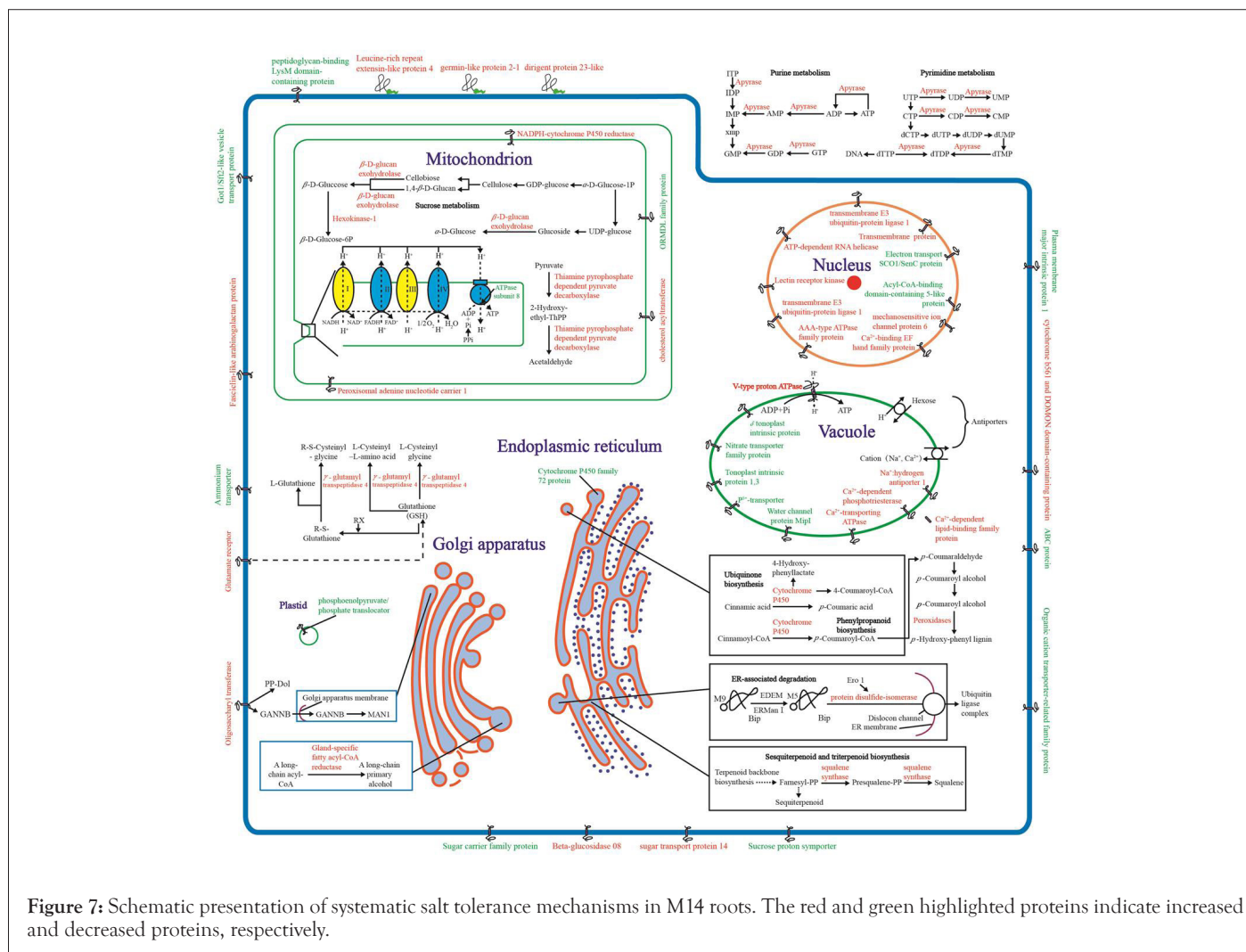


Figure 7: Schematic presentation of systematic salt tolerance mechanisms in M14 roots. The red and green highlighted proteins indicate increased and decreased proteins, respectively.

DISCUSSION

Using iTRAQ LC-MS/MS, we have identified and quantified many proteins from the sugar beet M14 plants under control and salt stress conditions. Many of the proteins are membrane proteins with diverse functions, such as transport, metabolism, signaling and energy. Here we focus on discussing membrane protein changes toward understanding the salt stress mechanisms of the M14 roots.

Transport and energy related proteins

Root is the initial organ to sense salt stress in soil. Since the main function of roots is to transport of water and nutrients, it is reasonable that the largest functional category of the membrane protein is transport-related. In this work, we identified 37 differentially expressed membrane proteins associated with the transport, with 24 increased and 13 decreased compared to the control (Table 1). It is known that Na⁺ in the roots is transported out by plasma membrane Na⁺/H⁺ antiporter or is transported into vacuoles through vacuolar Na⁺/H⁺ antiporter. Interestingly, we identified a Na⁺/H⁺ antiporter with two-fold increase under 400 mM NaCl treatment (Table 1). However, it appears to be

targeted to chloroplast thylakoid membrane. It is not known how this Na⁺/H⁺ antiporter contributes to salt tolerance. Another transporter that displayed a 2.8 fold increase under 400 mM NaCl is a sugar transport protein 13 (gi|590657945). Sugar can function as a signaling molecule and/or provides energy to enhance plant stress tolerance [37]. In addition, an ABCG/PDR subfamily ATP binding cassette (ABC) protein (gi|375273925) showed a 3.2 fold increase under salt stress. The ABC transporter superfamily proteins form a large and ubiquitous protein family. In previous studies, the functions of different members were found to be redundant [38,39]. In Arabidopsis, there are more than one hundred ABC transporters [40]. The genome size of rice is about 3.5 times that of Arabidopsis, but it has almost the same number of ABC transporter genes [41]. The original function of this transporter was associated with detoxification [42]. The ABC transporters have been found to involve in many biological processes, such as hormone transport, stomatal movement, metabolite transport and response to environmental stresses [43]. It was reported that ABC proteins can form homo-dimers to mediate abscisic acid (ABA) transport across the membrane under abiotic stresses [44]. Nevertheless, its function in glycophytes

is mainly focused on glutathione conjugate and chlorophyll catabolite transport, heme transport and helC homologue [45-47]. In salt stress proteomics of Arabidopsis [48,49] and rice [50,51], members of the ABC transporters were not found. Interestingly, in halophytes (e.g., *Suaeda salsa*), ABC transporter 1 is increased in both salt and heat shock stress [52]. Although ABC transporters appear to be important for halophytes, this protein was not found in leaf membrane proteomics of sugar beet M14 [14], but it was identified in the roots here. This evidence suggests that the ABC transporters may have different functions in glycophytes and halophytes. For halophytes, ABC transporters may play an important role in salt stress tolerance in a tissue-specific manner.

In addition to ABC transporter that use ATP directly for transport, here we identified five differentially expressed membrane proteins associated with energy and transport, four increased and one decreased in response to the salt stress treatments (Table 1). AAA-type ATPase family protein (gi|566206055) can hydrolyze ATP and transfer energy to target proteins, resulting in extensive conformational changes. In addition, a variety of specific adapter proteins can simultaneously control the conformation of AAA proteins and transfer energy to their target proteins [53]. V-ATPases (gi|733214298) in vacuolar membrane hydrolyze ATP to produce transmembrane electrochemical gradient, which drives a variety of cations (e.g., Na⁺) to accumulate into the vacuoles in order to maintain cell turgor, ion balance and promote plant growth under salt stress [54].

As to decreased transporters, three aquaporins, PIP1 (gi|1402833), MipI (gi|4884866) and TIP1.3 (gi|590563830), showed decreases in the M14 roots under salt stress. They transport water, and are involved in plant osmotic stresses (e.g., drought and high salt) [55]. The decreases of these proteins may reflect the capability of the M14 roots in maintaining water in the root cells [56,57].

Metabolism and signaling related proteins

Under salt stress, 32 differentially expressed membrane proteins associated with metabolism, including thirty increased and two decreased proteins (Table 1). First, NADPH-cytochrome P450 reductase provides electrons for cytochrome P450s in response to salt stress, and cytochrome P450s are involved in a variety of pathways involving oxidative metabolisms (e.g., synthesis of defensive metabolites) [58]. Second, beta-D-glucan exohydrolase family protein (gi|566232333) can hydrolyze glycosidic bonds between two or more carbohydrates and between carbohydrates and non-carbohydrate molecules [59]. Third, beta-glucosidase 8 (gi|350534796) can hydrolyze biologically inactive ABA-glucose ester to produce active ABA. It cooperates with ABA de novo synthesis to regulate cellular ABA levels in the course of plant growth and response to environmental stresses [60]. Fourth, cholesterol acyltransferase (gi|566161131) is one of the major enzymes involved in lipid metabolism, and may catalyze the transfer of acyl groups from lecithin to sterol, stabilizing the number of free sterols in the membrane [61]. Phytosterols are

important components of plant plasma membrane. The increased cholesterol acyltransferase may enhance membrane stability, thereby enabling the M14 salt stress tolerance. Fifth, hexokinase-1 (gi|11386885), which acts on hexose phosphorylation, is one of the key enzymes in the process of plant respiration and metabolism, and has been found to play a vital role in plant sugar signaling [62,63]. Most of the hexokinase-1 activity is associated with intracellular membranes. Such specific localization may be favorable for their involvement in compartmentalized metabolism or signal transduction [64,65].

Signal transduction plays an important role in plant salt stress response and tolerance [66]. Here we identified eight differentially expressed membrane proteins associated with the signaling, and they were increased under salt stress compared with control plants (Table 1). One of the proteins is calcium-binding EF hand family protein (gi|566182885), which increased 2.5 times. Calcium-binding EF hand family protein is involved in plant stress response through calcium signaling. As a calmodulin, it has 2-6 EF-hands motifs, the EF-hand motifs bind to Ca²⁺ through helix-loop-helix [67]. Another signaling protein is a lectin receptor kinase (gi|914726339). This group of kinases plays important roles in saccharide signaling, stress perception and plant innate immunity [68]. Its function in plant salt stress response has not been reported.

Correlation between transcript, protein and metabolite levels

Out of the 10 genes encoding differentially expressed membrane proteins in different functional categories, seven showed positive correlations between transcript and protein levels, and three showed opposite trends of changes (Table 2). The opposite trends could be attributed to differential regulation at transcriptional, posttranscriptional and posttranslational levels, as well as differential life-time and stability of the transcripts and proteins [69].

To test whether the changes of the differentially expressed proteins correlate with related metabolites, we measured the contents of glucose and GSH under 0 mM, 200 mM and 400 mM NaCl (Figure 6). GSH is not only a pivotal component of the glutathione-ascorbate cycle, but also the precursor of phytochelatin and glutathione oligomers that chelate heavy metals such as cadmium. In addition, small oxidoreductases such as glutaredoxins use GSH as a substrate [70,71]. Interesting, both GSH and a glutamate receptor protein (gi|590571602) were increased under the 200 mM and 400 mM NaCl treatments. The glutamate receptor protein may be likely to regulate GSH levels under salt stress in the M14 plants [36]. As to glucose, its decreased levels could be attributed to decreased photosynthesis and increased energy consumption under salt stress, e.g., for metabolism and membrane transport activities (see previous sections). The increase of beta-D-glucan exohydrolase found in proteomics did not contribute to the changes of glucose, highlighting the importance of molecular analyses at different levels.

Overview of membrane protein functions in M14 salt stress tolerance

A previous leaf membrane proteomics work of the M14 plants under salt stress (200 mM and 400 mM NaCl) revealed 30 increased and 10 decreased proteins compared to control, and the proteins were mainly localized in chloroplast and mitochondria [14]. While here the differentially expressed membrane proteins in the M14 roots are mainly localized in the nucleus, vacuole and mitochondria. The differences in the distribution may reflect the functions and relative abundances of membrane proteins in roots and leaves (Figure 7). Interestingly, a differentially expressed membrane protein dolichyl-diphospho oligosaccharide-protein glycosyltransferase (gi|590703969) was observed in both roots and leaves of the M14. It had about two-fold increases in the two tissues of M14 under salt treatments, suggesting protein glycosylation may constitute an important posttranslational modification (PTM) in the M14 salt stress tolerance. Table 1 summarizes root salt-responsive membrane proteins in different organelles including nucleus, vacuoles and mitochondria. For example, the increase of apyrase (gi|117622284) involved in purine and pyrimidine metabolism in the extracellular matrix is really interesting [72]. In addition to energy metabolism, the extracellular nucleotides (e.g., adenosine, ADP and ATP) can regulate ROS production, membrane channel activity and auxin transport [73-75]. The decrease of root growth under salt treatment (Figure 1) may be attributed to the inhibition of polar auxin transport caused by extracellular ATP and apyrase activity [75], which pose a negative regulatory role in the growth of plant roots. The functions of many interesting proteins discovered in this study deserve further investigation.

CONCLUSION

The iTRAQ LC-MS/MS based quantitative proteomics identified 343 unique membrane proteins in the roots of sugar beet M14 line. A total of 115 proteins exhibited significant changes in response to salt stress, with 96 increased and 19 decreased in protein levels (fold change >2 or <0.5, $p < 0.05$). The salt responsive membrane proteins were mainly involved in transport, signaling, stress and defense, and energy, and most of them were located in the vacuolar membrane, nuclear membrane, plasma membrane and mitochondrial membrane. Many interesting salt-stress responsive membrane proteins were discovered in the M14 roots, e.g., aquaporins, ABC transporter, Ca²⁺-binding protein, lectin receptor kinase, glutamate receptor and apyrase. Compared with glycophytes, sugar beet M14 ABC transporters from different subfamilies may play important roles in salt stress tolerance. The increase of a dolichyl-diphospho oligosaccharide glycosyltransferase in both root and leaf membrane proteomes highlights the importance of protein glycosylation in plant salt stress tolerance. Future studies on protein PTMs in the M14 will enhance understanding of the regulatory mechanisms important for plant salt stress signaling and tolerance.

ACKNOWLEDGEMENT

This research was supported by the National Science Foundation of China (Project 31471552: The response of antioxidant enzymes to salt stress in sugar beet M14, Project 31671751: Regulatory mechanisms of BvM14-glyoxalase I transcription factor involved in the response to salt stress, Project 31501359: Study on phosphorylation sites of a Ser/Thr protein kinase from sugar beet M14 line in response to salt stress and Project 31401441: Identification of root variation related proteins in sugar beet (*Beta vulgaris* L.) monosomic addition line M14 using LC-MS/MS analysis) and the National Science Foundation of Heilongjiang Province (Project C2015026), and the Common College Science and Technology Innovation Team of Heilongjiang Province (Project 2014TD004). The authors thank Daniel Chen from Honors College, Biomedical Sciences Program, University of South Florida for critical reading and editing of the manuscript.

REFERENCES

- Munns R, Tester M. Mechanisms of salinity tolerance. *Ann Rev Plant Biol.* 2008;59:651-681.
- Krishnamurthy P, Tan XF, Lim TK, Lim TM, Kumar PP, Loh CS, et al. Proteomic analysis of plasma membrane and tonoplast from the leaves of mangrove plant *Avicennia officinalis*. *Proteomics.* 2014;14:2545-2557.
- Hill CB, Cassin A, Keeble-Gagnere G, Doblin MS, Bacic A, Roessner U, et al. De novo transcriptome assembly and analysis of differentially expressed genes of two barley genotypes reveal root-zone-specific responses to salt exposure. *Sci Rep.* 2016;6:31558.
- Kazachkova Y, Khan A, Acuna T, Lopez-Diaz I, Carrera E, Khozin-Goldberg I, et al. Salt induces features of a dormancy-like state in seeds of eutrema (*Thellungiella*) *salsugineum*, a halophytic relative of *Arabidopsis*. *Frontiers in plant science* 2016, 7, 1071.
- Marsalova L, Vitamvas P, Hynek R, Prasil IT, Kosova K. Proteomic response of *hordeum vulgare* cv. *tadmor* and *hordeum marinum* to salinity stress: Similarities and differences between a glycophyte and a halophyte. *Front Plant Sci.* 2016;7:1154.
- Park YR, Choi MJ, Park SJ, Kang H. Three zinc-finger RNA-binding proteins in cabbage (*Brassica rapa*) play diverse roles in seed germination and plant growth under normal and abiotic stress conditions. *Physiol Plant.* 2016.
- Wang T, McFarlane HE, Persson S. The impact of abiotic factors on cellulose synthesis. *J Exp Bot.* 2016;67:543-552.
- Arya D, Kapoor S, Kapoor M. *Physcomitrella patens* DNA methyltransferase 2 is required for recovery from salt and osmotic stress. *FEBS J.* 2016;283:556-570.
- Sudan J, Negi B, Arora S. Oxidative stress induced expression of monodehydroascorbate reductase gene in *Eleusine coracana*. *FEBS J.* 2015;21(4):551-558.
- Liu WZ, Deng M, Li L, Yang B, Li H, Deng H, et al. Rapeseed calcineurin B-like protein CBL4, interacting with CBL-interacting protein kinase CIPK24, modulates salt tolerance in plants. *Biochem Biophys Res Comm.* 2015;467(3):467-471.

11. Li W, Zhao F, Fang W, Xie D, Hou J, Yang X, et al. Identification of early salt stress responsive proteins in seedling roots of upland cotton (*Gossypium hirsutum* L.) employing iTRAQ-based proteomic technique. *Front Plant Sci.* 2015;6:732.
12. Li H, Cao H, Wang Y, Pang Q, Ma C, Chen S, et al. Proteomic analysis of sugar beet apomictic monosomic addition line M14. *J Proteomics.* 2009;73(2):297-308.
13. Yang L, Ma C, Wang L, Chen S, Li H. Salt stress induced proteome and transcriptome changes in sugar beet monosomic addition line M14. *J Plant Physiol.* 2012;169(9):839-850.
14. Li H, Pan Y, Zhang Y, Wu C, Ma C, Yu B, et al. Salt stress response of membrane proteome of sugar beet monosomic addition line M14. *J proteomics.* 2015;127:18-33.
15. Yang L, Zhang Y, Zhu N, Koh J, Ma C, Pan Y, et al. Proteomic analysis of salt tolerance in sugar beet monosomic addition line M14. *J Proteome Res.* 2013;12(11):4931-4950.
16. Yu B, Li J, Koh J, Dufresne C, Yang N, Qi S, et al. Quantitative proteomics and phosphoproteomics of sugar beet monosomic addition line M14 in response to salt stress. *J Proteomics.* 2016;143:286-297.
17. Yuan Y, Zhong M, Shu S, Du N, Sun J, Guo S, et al. Proteomic and physiological analyses reveal putrescine responses in roots of cucumber stressed by NaCl. *Front Plant Sci.* 2016;7:1035.
18. Contreras-Cornejo HA, Macias-Rodriguez L, Alfaro-Cuevas R, Lopez-Bucio J. *Trichoderma* spp. Improve growth of *Arabidopsis* seedlings under salt stress through enhanced root development, osmolite production, and Na(+) elimination through root exudates. *MPMI.* 2014;27(6):503-514.
19. Campo S, Baldrich P, Messeguer J, Lalanne E, Coca M, San Segundo B, et al. Overexpression of a calcium-dependent protein kinase confers salt and drought tolerance in rice by preventing membrane lipid peroxidation. *Plant Physiol.* 2014;165(2):688-704.
20. Nozawa A, Tozawa Y. Modifications of wheat germ cell-free system for functional proteomics of plant membrane proteins. *Methods Mol Biol.* 2014;1072:259-272.
21. Baunsgaard L, Fuglsang AT, Jahn T, Korthout HA, de Boer AH, Palmgren MG, et al. The 14-3-3 proteins associate with the plant plasma membrane H(+)-ATPase to generate a fusicoccin binding complex and a fusicoccin responsive system. *Plant Journal.* 1998;13(5):661-671.
22. Reed JR, Backes WL. The functional effects of physical interactions involving cytochromes P450: Putative mechanisms of action and the extent of these effects in biological membranes. *Drug Metabol Rev.* 2016;25:1-58.
23. Kota U, Goshe MB. Advances in qualitative and quantitative plant membrane proteomics. *Phytochem.* 2011;72(10):1040-1060.
24. Gilmore JM, Washburn MP. Advances in shotgun proteomics and the analysis of membrane proteomes. *J Proteomics.* 2010;73(11):2078-2091.
25. Gomes BR, Siqueira-Soares Rde C, Dos Santos WD, Marchiosi R, Soares AR, Ferrarese-Filho O, et al. The effects of dopamine on antioxidant enzymes activities and reactive oxygen species levels in soybean roots. *Plant Signal Behav.* 2014;9(12):e977704.
26. Koh J, Chen G, Yoo MJ, Zhu N, Dufresne D, Erickson JE, et al. Comparative proteomic analysis of *Brassica napus* in response to drought stress. *J Proteome Res.* 2015;14(8):3068-3081.
27. Ma H, Xu X, Feng L. Responses of antioxidant defenses and membrane damage to drought stress in fruit bodies of *Auricularia auricula-judae*. *World J Microbiol Biotechnol.* 2014;30(1):119-124.
28. Gupta AS, Webb RP, Holaday AS, Allen RD. Overexpression of superoxide dismutase protects plants from oxidative stress (induction of ascorbate peroxidase in superoxide dismutase-overexpressing plants). *Plant Physiol.* 1993;103(4):1067-1073.
29. Washburn MP. The H-index of 'an approach to correlate tandem mass spectral data of peptides with amino acid sequences in a protein database'. *J Am Soc Mass Spectrom.* 2015;26(11):1799-1803.
30. Untergasser A, Nijveen H, Rao X, Bisseling T, Geurts R, Leunissen JA, et al. Primer3Plus, an enhanced web interface to Primer3. *Nucleic Acids Res.* 2007;35:W71-W74.
31. Rozen S, Skaletsky H. Primer3 on the WWW for general users and for biologist programmers. *Meth Mol Biol.* 2000;132:365-386.
32. Smith IK, Vierheller TL, Thorne CA. Assay of glutathione reductase in crude tissue homogenates using 5,5'-dithiobis(2-nitrobenzoic acid). *Analyt Biochem.* 1988;175(2):408-413.
33. Solari FA, Matheij NJ, Burkhart JM, Swieringa F, Collins PW, Cosemans JM, et al. Combined quantification of the global proteome, phosphoproteome and proteolytic cleavage to characterize altered platelet functions in the human Scott syndrome. *Mol cell Proteomics MCP.* 2016.
34. Zou JJ, Zheng ZY, Xue S, Li HH, Wang YR, Le J, et al. The role of *Arabidopsis* actin-related protein 3 in amyloplast sedimentation and polar auxin transport in root gravitropism. *J Experiment Bot.* 2016.
35. Pompella A, Visvikis A, Paolicchi A, De Tata V, Casini AF. The changing faces of glutathione, a cellular protagonist. *Biochem Pharmacol.* 2003;66(8):1499-1503.
36. Zou JJ, Zheng ZY, Xue S, Li HH. Glutamate receptor-like channel3.3 is involved in mediating glutathione-triggered cytosolic calcium transients, transcriptional changes, and innate immunity responses in *Arabidopsis*. *Plant Physiol.* 2008;162:1497-1509.
37. Chiou TJ, Bush DR. Sucrose is a signal molecule in assimilate partitioning. *Proceedings of the National Academy of Sciences of the United States of America.* 1998;95(8):4784-4788.
38. Wanke D, Üner Kolukisaoglu H. An update on the ABCC transporter family in plants: many genes, many proteins, but how many functions? *Plant Biol.* 2010;12:15-25.
39. Lefevre F, Bajiot A, Boutry M. Plant ABC transporters: time for biochemistry? *Biochem Soc Trans.* 2015;43:931-936.
40. Sánchez-Fernández RO, Davies TE, Coleman JO, Rea PA. The *Arabidopsis thaliana* ABC protein superfamily, a complete inventory. *J Biol Chem.* 2001;276:30231-30244.
41. Garcia O, Bouige P, Forestier C, Dassa E. Inventory and comparative analysis of rice and *Arabidopsis* ATP-binding cassette (ABC) systems. *J Mol Biol.* 2010;343:249-265.
42. Martinoia E, Klein M, Geisler M, Bovet L, Forestier C, Kolukisaoglu Ü, et al. Multifunctionality of plant ABC transporters—more than just detoxifiers. *Planta.* 2002;214:345-355.

43. Kretschmar T, Kohlen W, Sasse J, Borghi L, Schlegel M, Bachelier JB, et al. A petunia ABC protein controls strigolactone-dependent symbiotic signalling and branching. *Nature*. 2012;483(7389):341-344.
44. Kuromori T, Miyaji T, Yabuuchi H, Shimizu H, Sugimoto E, Kamiya A, et al. ABC transporter AtABCG25 is involved in abscisic acid transport and responses. *Proc Natl Acad Sci U S A*. 2010;107(5):2361-2366.
45. Lu YP, Li ZS, Drozdowicz YM, Hörtensteiner S, Martinoia E, Rea PA, et al. AtMRP2, an Arabidopsis ATP binding cassette transporter able to transport glutathione S-conjugates and chlorophyll catabolites: functional comparisons with AtMRP1. *Plant Cell*. 1998;10:267-282.
46. Nakazono M, Ito Y, Tsutsumi N, Hirai A. The gene for a subunit of an ABC-type heme transporter is transcribed together with the gene for subunit 6 of NADH dehydrogenase in rice mitochondria. *Curr Genet*. 2006;29:412-416.
47. Sánchez-Fernández R, Ardiles-Díaz W, Van Montagu M, Inzé D, May M. Cloning and expression analyses of AtMRP4, a novel MRP-like gene from *Arabidopsis thaliana*. *Mol Gen Genet*. 1998;258:655-662.
48. Jiang Y, Yang B, Harris NS, Deyholos MK. Comparative proteomic analysis of NaCl stress-responsive proteins in *Arabidopsis* roots. *J Experiment Bot*. 2007;58:3591-3607.
49. Pang Q, Chen S, Dai S, Chen Y, Wang Y, Yan X. Comparative proteomics of salt tolerance in *Arabidopsis thaliana* and *Thellungiella halophila*. *J Proteome Res*. 2010;9:2584-2599.
50. Yan S, Tang Z, Su W, Sun W. Proteomic analysis of salt stress-responsive proteins in rice root. *Proteomics*. 2005;5:235-244.
51. Chitteti BR, Peng Z. Proteome and phosphoproteome differential expression under salinity stress in rice (*Oryza sativa*) roots. *J Proteome Res*. 2007;6:1718-1727.
52. Li W, Zhang C, Lu Q, Wen X, Lu C. The combined effect of salt stress and heat shock on proteome profiling in *Suaeda salsa*. *J Plant Physiol*. 2011;168:1743-1752.
53. Jentsch S, Rumpf S. Cdc48 (p97): A "molecular gearbox" in the ubiquitin pathway? *Trends Biochem Sci*. 2007;32(1):6-11.
54. Lehr A, Kirsch M, Viereck R, Schiemann J, Rausch T. cDNA and genomic cloning of sugar beet V-type H⁺-ATPase subunit A and c isoforms: Evidence for coordinate expression during plant development and coordinate induction in response to high salinity. *Plant Mol Biol*. 1999;39(3):463-475.
55. Maurel C, Verdoucq L, Luu DT, Santoni V. Plant aquaporins: Membrane channels with multiple integrated functions. *An Rev Plant Biol*. 2008;59:595-624.
56. Hachez C, Veselov D, Ye Q, Reinhardt H, Knipfer T, Fricke W, et al. Short-term control of maize cell and root water permeability through plasma membrane aquaporin isoforms. *Plant Cell Env*. 2012;35(1):185-198.
57. Kirch HH, Vera-Estrella R, Gollmack D, Quigley F, Michalowski CB, Barkla BJ, et al. Expression of water channel proteins in *Mesembryanthemum crystallinum*. *Plant Physiol*. 2000;123(1):111-124.
58. Zhang Y, Wang Y, Wang L, Yao J, Guo H, Fang J, et al. Knockdown of NADPH-cytochrome P450 reductase results in reduced resistance to buprofezin in the small brown planthopper, *Laodelphax striatellus* (fallen). *Pesticide Biochem Physiol*. 2016;127:21-27.
59. Luang S, Hrmova M, Ketudat Cairns JR. High-level expression of barley beta-D-glucan exohydrolase HvExoI from a codon-optimized cDNA in *Pichia pastoris*. *Protein Exp Pur*. 2010;73(1):90-98.
60. Aoki K, Yano K, Suzuki A, Kawamura S, Sakurai N, Suda K, et al. Large-scale analysis of full-length cDNAs from the tomato (*Solanum lycopersicum*) cultivar micro-tom, a reference system for the solanaceae genomics. *BMC Genomics*. 2010;11:210.
61. Banas A, Carlsson As Fau-Huang B, Huang B, Fau-Lenman M, Lenman M, Fau-Banas W, et al. Cellular sterol ester synthesis in plants is performed by an enzyme (phospholipid:sterol acyltransferase) different from the yeast and mammalian acyl-CoA:sterol acyltransferases. *J Biol Chem*. 2005;14:280.
62. Kim YM, Heinzel N, Giese JO, Koeber J, Melzer M, Rutten T, et al. A dual role of tobacco hexokinase 1 in primary metabolism and sugar sensing. *Plant Cell Env*. 2013;36:7.
63. Claeysen E, Rivoal J. Isozymes of plant hexokinase: Occurrence, properties and functions. *Phytochem*. 2007;68:6.
64. Frommer WB, Schulze W, Fau-Lalonde S, Lalonde S. Plant science. Hexokinase, jack-of-all-trades. *Sci*. 2003;300(5617):261-263.
65. Moore B, Zhou L, Fau-Rolland F, Fau-Hall Q. Role of the arabidopsis glucose sensor HXK1 in nutrient, light, and hormonal signaling. *PLoS one*. 2016.
66. Zhu JK. Salt and drought stress signal transduction in plants. *Annual Rev Plant Biol*. 2002;53:247-73.
67. Chen C, Sun X, Duanmu H, Zhu D, Yu Y, Cao L, et al. GsCML27, a gene encoding a calcium-binding ef-hand protein from Glycine soja, plays differential roles in plant responses to bicarbonate, salt and osmotic stresses. *PLoS one*. 2015;10(11):e0141888.
68. Wang Y, Weide R, Govers F, Bouwmeester K. L-type lectin receptor kinases in *Nicotiana benthamiana* and tomato and their role in phytophthora resistance. *J Exp Botany*. 2015;66(21):6731-6743.
69. Walley JW, Sartor RC, Shen Z, Schmitz RJ, Wu KJ, Ulrich MA, et al. Integration of omic networks in a developmental atlas of maize. *Science*. 2016;353:814-818.
70. Nocto G, Foyer CH. Ascorbate and glutathione: keeping active oxygen under control. *Ann Rev Plant Physiol Plant Mol Biol*. 1998;49:249-279.
71. Rouhier N, Lemaire SD, Jacquot JP. The role of glutathione in photosynthetic organisms: Emerging functions for glutaredoxins and glutathionylation. *Ann Rev Plant Biol*. 2008;59:143-166.
72. Reichler SA, Torres J, Rivera AL, Cintolesi VA, Clark G, Roux SJ. Intersection of two signalling pathways: extracellular nucleotides regulate pollen germination and pollen tube growth via nitric oxide. *J Experiment Botany*. 2009;60(7):2129-2138.
73. Song CJ, Steinebrunner I, Wang X, Stout SC, Roux SJ. Extracellular ATP induces the accumulation of superoxide via NADPH oxidases in *Arabidopsis*. *Plant Physiol*. 2006;140(4):1222-1232.
74. Demidchik V, Shang Z, Shin R, Thompson E, Rubio L, Laohavisit A, et al. Plant extracellular ATP signalling by plasma membrane NADPH oxidase and Ca²⁺ channels. *Plant J Cell Mol Biol*. 2009;58(6):903-913.
75. Tang W, Brady SR, Sun Y, Muday GK, Roux SJ. Extracellular ATP inhibits root gravitropism at concentrations that inhibit polar auxin transport. *Plant Physiol*. 2003;131(1):147-154.